Mon. Not. R. Astron. Soc. **000**, 1–?? (2002) Printed 29 November 2016 (MN LATEX style file v2.2)

# Broad Band X-ray Spectra of Atoll Source 4U 1636-536: NuSTAR and Swift Results

V. K. Agrawal[1⋆] and Mohammad Hasan[1]
[1] *Space Astronomy Group, ISRO Satellite Center, ISITE Campus,Bangalore 560037,INDIA*



29 November 2016

**ABSTRACT**

In this work we investigate broad band (1-79 keV) spectral nature of the atoll source 4U 1636-536 using the combined Nu-STAR and SWIFT-XRT data. The spectra are complex and have emission components from the disc, boundary-layer and corona. In addition to that a broad iron line is also observed. A relativistic line model assuming Schwarzchild metric fits this feature. The total flux varies from 1.4 $\times$ $10^{-9}$ to 4.36 $\times$ $10^{-9}$ $ergs/s/cm^2$. At the highest flux level the source was found in the soft state. In this state the Comptonized component has temperature $kT_e \sim 3$ keV and optical depth $\tau \sim 16$. We also detect a non-thermal tail with index $\sim 2.4$, contributing $\sim 10$ % of the total flux in the soft state. We also find that the inner disc radius, electron temperature and optical depth vary with the total 0.1-100 keV unabsorbed flux. We discuss the implication of the results in this paper.

**Key words:** accretion, accretion discs - X-rays: binaries - X-rays: individual: 4U 1636-536

## 1 INTRODUCTION

Low magnetic field neutron stars in low-mass X-ray binaries (LMXBs) are of great interest due to the fact that they provide an excellent laboratory to study the properties of matter at extreme densities. They are broadly divided in two classes: Atoll source and Z-source based on their correlated spectral and timing properties (Hasinger and van der Klis 1989).

Atoll sources trace fragmented path in the Color-Color diagram (CD). They have luminosity in the range of 0.01-0.2 $L_{Edd}$ (Done et al. 2007). The atoll-track consists of an upwardly curved branch at the right hand side of the CD, called 'banana' branch and bunch of uncorrelated points in the left hand side called 'island state'.

The source 4U 1636-536 is one of the well studied atoll source. The source has exhibited Quasi-Periodic-Oscillations (Wijnands et al. 1997). type-I X-ray bursts (Galloway et al. 2006) and millisecond oscillations during thermonuclear bursts (Strohmayer & Markwardt 2002). The orbital period of the source is $\sim$ 3.8 hr (Giles et al. 2002). The optical observations suggest that inclination lies in the range $\sim 30-60^{\circ}$ (Casares et al. 2006). The distance to the source has been estimated to be 6.0$\pm$0.5 kpc (Galloway et al. 2006).

X-ray spectra of neutron star LMXBs are in general complex and have multiple emission components, arising in different regions of the accretion flow. The complex spectra have two main components, soft and hard. Two different approach have been adopted to fit the X-ray spectra of neutron star LMXBs. In first approach, the soft component is modeled as multicolor-disc-blackbody (MCD) (Mitsuda et al. 1984, 1989), coming from optically thick accretion disc and the hard component is described by Comptonized emission from the boundary-layer (Agrawal and Sreekumar 2003; Agrawal and Misra 2009; Di Salvo et al. 2002; Barret 2001; Barret et al. 2000; Tarana,Bazzano, Ubertini 2008). In second approach, the soft component is modeled as blackbody emission from the hot surface of neutron star and the hard Comptonized component is considered to be arising from the hot inner flow (Di Salvo et al. 2000; Barret 2001; Barret et al. 2000; Sleator et al. 2016). However, combination of two thermal components (Blackbody and MCD) and Comptonized emission have also been used to model the X-ray spectra of atoll sources Ser X-1 ( Chiang et al. 2016; Miller et al. 2013) and 4U 1636-536 (Sanna et al. 2013; Lyu et al. 2014).

Spectra of Z-sources are generally soft. The Comptonized component has temperatures in the range of 2-5 keV and the optical depth in the range of 10-20 for a spherical geometry of the corona (Agrawal and Misra 2009; Barret 2001). Atoll sources exhibit two types of state: hard and

⋆ E-mail: vivekag@isac.gov.in

**Table 1.** NuSTAR and Swift observations of 4U 1636-536

| Obs | ObsID (NuSTAR) | Start Date (hh:mm:ss) | START UT (ksec) | Duration |
|---|---|---|---|---|
| 1 | 30101024002 | 2015-06-10 | 08:11:07 | 19.8 |
| 2 | 30102014002 | 2015-08-25 | 02:51:08 | 27.4 |
| 3 | 30102014004 | 2015-09-05 | 17:41:05 | 27.4 |
| 4 | 30102014006 | 2015-09-18 | 07:06:10 | 27.4 |
| Obs | ObsID (SWIFT) | Start Date (hh:mm:ss) | START UT (ksec) | Duration |
| 1 | 00081640002 | 2015-06-10 | 10:10:43 | 1.47 |
| 2 | 00081640003 | 2015-08-25 | 14:02:52 | 2.75 |
| 3 | 00081594001 | 2015-09-05 | 21:15:52 | 0.7 |
| 4 | 00081594002 | 2015-09-18 | 14:16:31 | 2.9 |

soft. In the soft state, spectra are similar to the Z-sources. However, in the hard state, the temperature of Comptonized component has a value in the range of 10-50 keV and some time extend beyond 100 keV (Piraino et al. 1999). In the hard state optical depth of the corona is found to be in the range of $\sim$ 2-4 for a spherical geometry of the corona (Barret 2001; Barret et al. 2000; Tarana,Bazzano, Ubertini 2008). During the soft state of atoll sources a hard power-law tail has also been observed ( Piraino et al. 2007; Tarana et al. 2011).

A part of hard X-rays from corona illuminates the accretion disc and gets reprocessed and reflected. The reflected emission consists of a Compton hump that peaks $\sim$ 10-40 keV and a relativistically smeared iron $K_\alpha$ line ( Fabian et al. 1989; Miller 2007; Reynolds and Nowak 2003). Relativistically smeared iron line have been observed in a few NS LMXBs with NuSTAR (eg. 4U 1728-34, Sleator et al. 2016; Serpens X-1 Miller et al. 2013; 4U 1608-522 Degenaar et al. 2015).

In this paper we present broad band spectra of neutron star low-mass X-ray binary 4U 1636-536. The broad spectra are analyzed using quasi-simultaneous data from SWIFT-XRT (1-10 keV) and NuSTAR (3-79 keV). In section 2 we present observation and data reduction procedure. In section 3 we provide analysis methodology and highlight the results. In section 4 we discuss the results of the spectral analysis.

## 2 OBSERVATION AND DATA REDUCTION

*NuSTAR* observed the atoll source 4U 1636-536 four times during June 2015 to Sep 2015. The observation log is shown in Table 1. The source was observed for a total duration of $\sim$ 106 ks. The data were processed using the NuSTAR Data Analysis Software (NuSTARDAS). The clean event files were created using *nupipeline*. A circular region of size $80''$ centered at the source position was created to extract the source spectra and light curves. The background events were extracted from a circular region away from the source with size similar to the source region. The standard FTOOL task *nuproducts* was used to create the spectra, lightcurves and response files.

Quasi-simultaneous Swift XRT data were also available in the archive (see Table 1). The swift data were taken in "windowed timing mode". We produced clean event and area response files using XRTPIPELINE software. From the clean events source events were extracted from a circular region of 20 pixels. The background events were extracted for an annular region with inner radius of 20 pixels and outer radius of 180 pixels. The spectra and light curves were extracted using XSELECT software. The backscale was set to 40 (twice the radius of circular source region) for the source spectra and to 160 (difference between inner and outer radius of annular region) for the background spectra. The count rate was below 100 counts/s for all the observations and hence spectra were pileup free.

Simultaneous XRT and NuSTAR spectra were fitted with spectral analysis package XSPEC (Arnaud and Dorman 2000). We used the latest calibration files to generate the response matrices. The spectra were grouped to give a minimum of 50 counts/bin. Unless quoted explicitly the error bars on the spectral parameters are computed using $\Delta\chi^2 = 1.0$.

## 3 ANALYSIS AND RESULTS

The investigation of background subtracted lightcurves revealed the presence of 13 type-I X-ray bursts. We have shown the lightcurves of all the observations after removing the type-I X-ray bursts for a comparison of persistent flux level (see Figure 1). We exclude the type-I X-ray bursts and fit the continuum spectral model to the persistent emission. We use the *tbabs* model (Wilms et al. 2000) to account for the interstellar absorption in the direction of 4U 1636-536. The neutral hydrogen column density (nH) in the direction of 4U 1636-536 is $\sim 4.1 \times 10^{21}$ and hence it is fixed at this value. The spectral fit is performed for the combined Swift-XRT data (1-9 keV) and NuSTAR spectra (3-79 keV). The Swift-XRT is poorly calibrated between the energy range 1.6-2.1 keV, hence we ignore the data between this energy range while performing the spectral modeling.

First we fit the combined data using the *diskbb* and the thermal Comptonization model. Basic thermal Comptonization models in XSPEC are : *CompST* (Sunyaev & Titarchuk 1980), *CompTT* ( Titarchuk 1994) and *nthComp* ( Zdziarski et al. 1996). The seed photons for inverse Compton scattering can be either single temperature blackbody emission arising in the surface of Neutron-Star/Boundary-Layer or Multi-color-disc component (MCD) from standard accretion disc. We use the *nthComp* model in XSPEC ( Zdziarski et al. 1996; Zycki et al. 1999) to describe the Comptonized emission from the corona. The reason for choosing *nthComp* model is that, this emission model provides a way to choose the source of the seed photons. We choose MCD as source of seed photons and tie the value of the seed photon temperature with the inner disc temperature. Then we add a single temperature blackbody (*bbodyrad* in XSPEC) component to account for the emission from the neutron star surface. The addition of this component improves the fit considerably. There is still some residual left around 4-7 keV suggesting Fe line component. An addition of Gaussian line component $\sim$ 6.4-6.7 keV improves the fit. We adopted similar procedure for other observations. We also try *diskline* model (see Fabian et al 1989) for a Schwarzschild metric to describe the broad iron line feature. This procedure was repeated for all the obser-

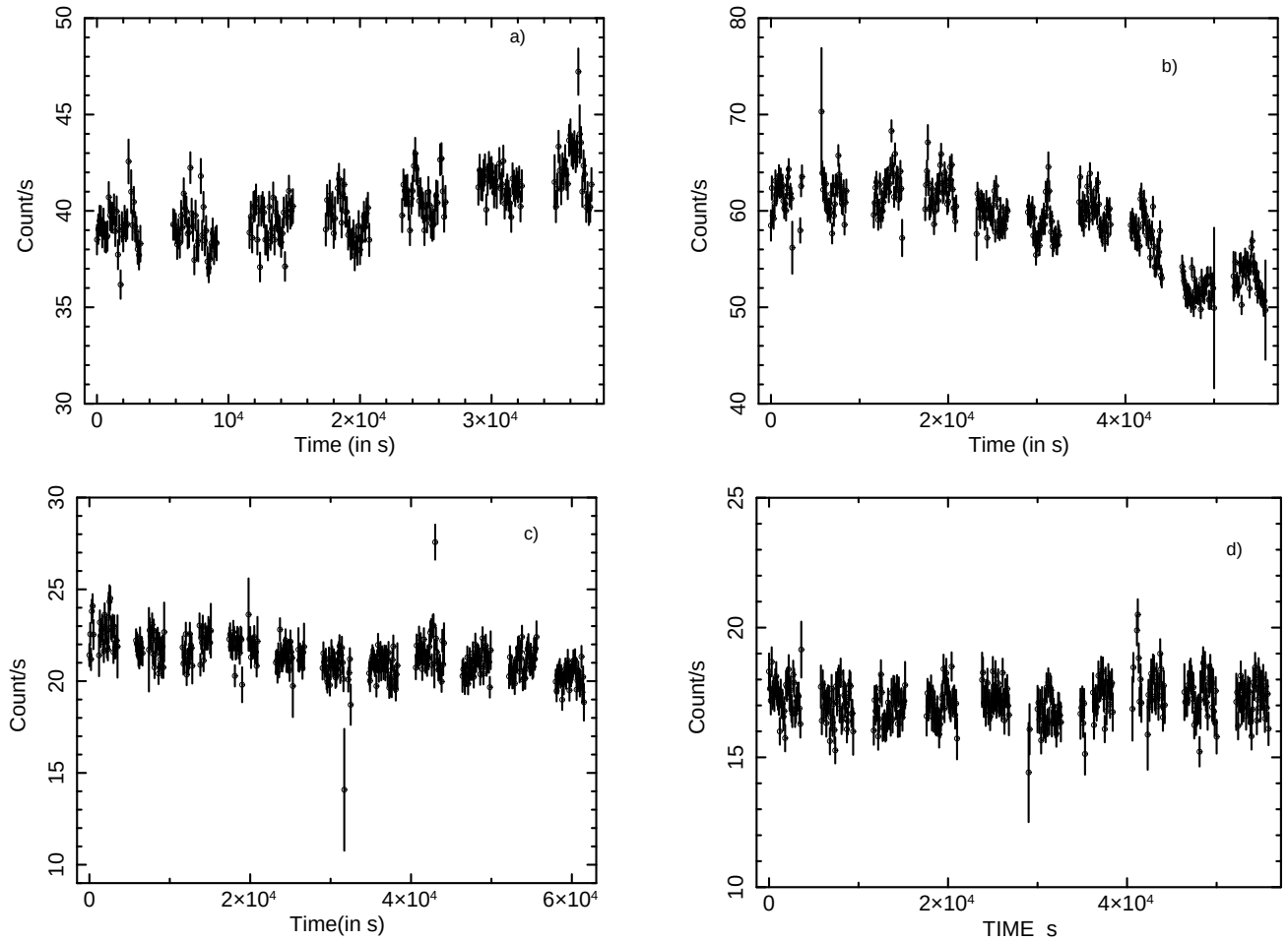


**Figure 1.** Lightcurves of the atoll source 4U 1636-536 as observed by NuSTAR. Figures a),b),c) and d) are the lightcurves for Obs-1,Obs-2,Obs-3 and Obs-4 respectively . The time bin used is 100 seconds. It is clear that the source is in the high-intensity state during Obs-2 (see Figure b above)

**Table 2.** In this table we give our approch to obtain the correct spectral model which fits the combined NuSTAR and Swift spectra.

| Model (tried) | $\chi^2_\nu$(Obs-1) | $\chi^2_\nu$(Obs-2) | $\chi^2_\nu$(Obs-3) | $\chi^2_\nu$(Obs-4) |
|---|---|---|---|---|
| diskbb+nthComp | 4.02 | 1.58 | 2.21 | 1.24 |
| diskbb+nthComp + bbodyrad | 1.16 | 1.18 | 1.25 | 1.07 |
| diskbb+nthComp + bbodyrad+gauss | 1.02 | 1.12 | 1.14 | 1.02 |
| diskbb+nthComp + bbodyrad+diskline | 1.05 | 1.14 | 1.16 | 1.02 |
| diskbb+nthComp + bbodyrad+Gauss+power-law | - | 1.07 | - | - |
| diskbb+nthComp + bbodyrad+diskline+power-law | - | 1.08 | - | - |

vations and results are given in Table 2. In Figure 2 we show the unfolded spectra for observation 1. For the second observation (OBSID 30102014002), a significant residual above 30 keV is observed (see Figure 3a ). This suggests the presence of an additional hard component in the spectrum. Hence we add a power-law component to remove this residual (see Figure 3b ). This further improves the fit. Therefore we consider $diskbb + nthComp + bbodyrad + diskline$ model as final description of the combined NuSTAR and SWIFT-XRT spectra except for OBSID 30102014002 where an additional power-law component is required.

The best fit spectral parameters for the final model are listed in Table 3. The source exhibits both soft and hard states during NuSTAR and SWIFT observations. During Obs-2 the source is found to be in the soft state. For this observation the corona temperature $kT_e$ is $\sim 3$ keV and the optical depth $\tau$ is $\sim 16$ . An additional non-thermal tail with photon index $\Gamma \sim 2.45$ is also present in this observation. For other three observations $kT_e$ is $\sim 10-20$ keV and $\tau$ is $\sim 4-5$.

The temperature of the soft disc component is found to be in the range of $\sim$ 0.5-0.9 keV. During the soft state the disc temperature is the highest (0.87$\pm$0.02 keV) suggesting that the disc has moved closer to the neutron star surface.

**Table 3.** In this table we give best-fit spectral fit parameters for combined NuSTAR-SWIFT observations. $kT_{in}$ is inner disk temperature and $N_{dbb}$ is normalization in XSPEC model *diskbb*. $R_{disk}$ is inner disc radius obtained using *diskline* model. $kT_{BB}$ is blackbody temperature and $N_{BB}$ is normalization of *bbodyrad* model. The parameters $kT_e$ is electron temperature and $\Gamma_c$ is power-law photon-index obtained from *nthComp* model. $\tau$ is optical depth estimated using $\Gamma_c$ and $kT_e$. $FWHM$ is full width-half maxima of Gaussian component. $EW$ is equivalent width of diskline component. $F_{tot}$ , $F_{Compt}$, ,$F_{pow}$ , $F_{dbb}$ $F_{bb}$ are total,Comptonized,power-law,disk-blackbody and blackbody 0.1-100 keV unabsorbed fluxes. All the fluxes are in the units of $10^{-9}$ $ergs/s/cm^2$.

| Parameters | Obs-1 | Obs-2 | Obs-3 | Obs-4 |
|---|---|---|---|---|
| $kT_{in}u$ (in keV) | 0.56±0.01 | 0.87±0.02 | 0.52±0.02 | 0.73±0.04 |
| $N_{dbb}$ | 388±18.6 | 204±7.5 | 320±23.2 | 49±2.1 |
| $R_{disk}$(in $R_g$) | 8.89±1.19 | 6.8±0.5 | $14.95^{+8.9}_{-2.7}$ | 24.9±4.6 |
| $kT_{BB}$ (in keV) | 1.69±0.02 | 1.54±0.03 | 1.39±0.02 | 1.23±0.04 |
| $N_{BB}$ | 3.4±00.41 | 15.45±0.42 | 4.6±0.45 | 2.66±0.35 |
| $\Gamma_c$ | 2.03±0.02 | 1.47±0.03 | 1.94±0.03 | 1.76±0.01 |
| $kT_e$ | 10.1±0.39 | 2.93±0.03 | 13.16±0.71 | 19.05±1.24 |
| $\tau$ | 4.65±0.11 | 16.45±0.72 | 4.30±0.18 | 4.03±0.29 |
| $FWHM$ (in keV) | 1.1±0.05 | 1.44±0.04 | 1.39±0.12 | 1.14±0.16 |
| EW(in eV) | 160 | 120 | 108 | 102 |
| $F_{tot}$ | 3.09±0.12 | 4.36±0.11 | 1.95±0.05 | 1.42±0.04 |
| $F_{Compt}$ | 1.81±0.09 | 0.67±0.08 | 1.04±0.04 | 0.977±0.08 |
| $F_{dbb}$ | 0.776±0.03 | 2.04±0. 05 | 0.457±0.03 | 0.213±0.01 |
| $F_{bb}$ | 0.436±0.02 | 1.20±0.06 | 0.438±0.02 | 0.239±0.02 |
| $F_{pow}$ | - | 0.416±0.009 | - | - |

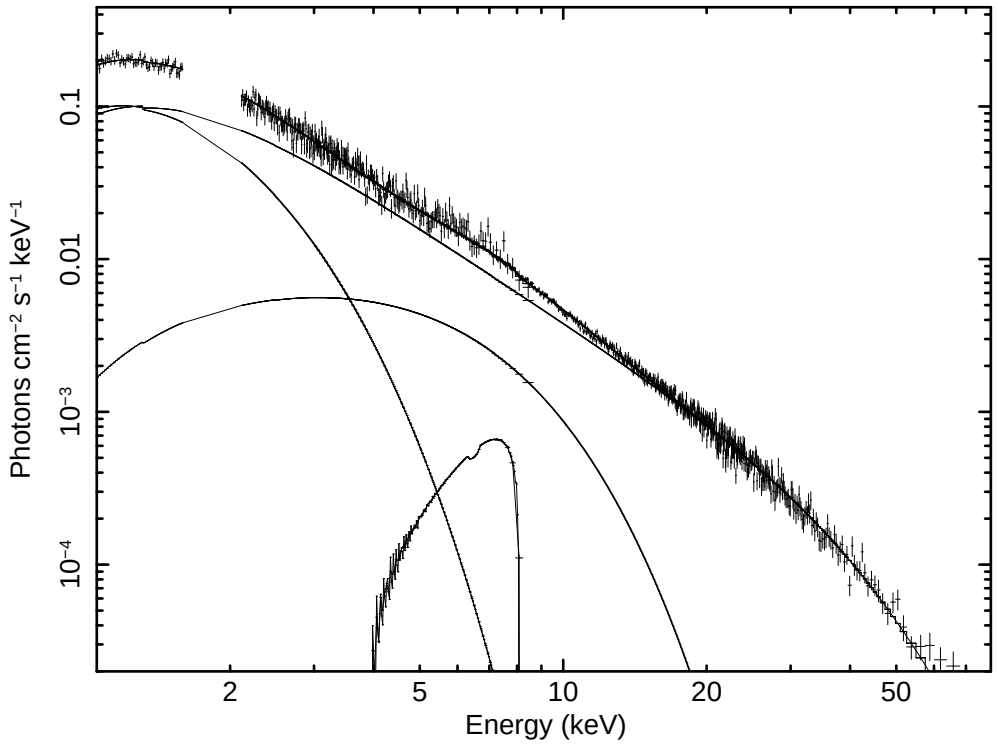


**Figure 2.** The unfolded spectrum for Obs-1. The spectral components are: *diskbb*,*diskline bbodyrad* and *nthComp*.

This is also evident from the fact that the inner disc radius derived from the *diskline* is $\sim$ 6.8 $GM/c^2$ i.e very close to ISCO (Inner-most stable circular orbit). The blackbody component has temperature in the range of $\sim$ 1.2-1.7 keV. The total flux is the highest during the soft state and hence we call it high-soft state.

A Gaussian iron line component seen in this source is very broad ($FWHM \sim 1.1 - 1.4$ keV) and strong. The iron line can also be described by *diskline* model which includes relativistic effect on the line emission for a non-rotating blackhole ( Fabian et al. 1989). We fix the emissivity index at $-3$ and the disc inclination at 60°. The equivalent width of the iron line is in the range of $\sim$ 100-160 eV. No correlation between iron line flux and total flux is observed. Modeling of the iron line with *diskline* model suggests that the disc is truncated. The truncation radius is anticorrelated with the total flux and varies from 6.8 to 25 $GM/c^2$ as the total flux decreases.

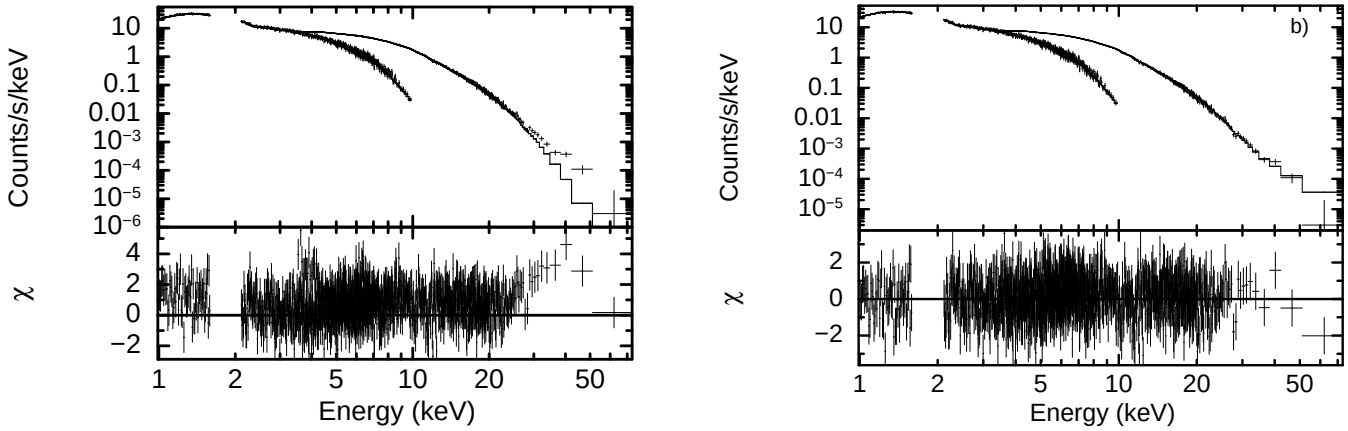


**Figure 3.** a) The data and best fit folded model for obs-2. It is clear from this figure that there is residual above 25 keV. b) Inclusion of power-law components remove the residual and improves the fit.

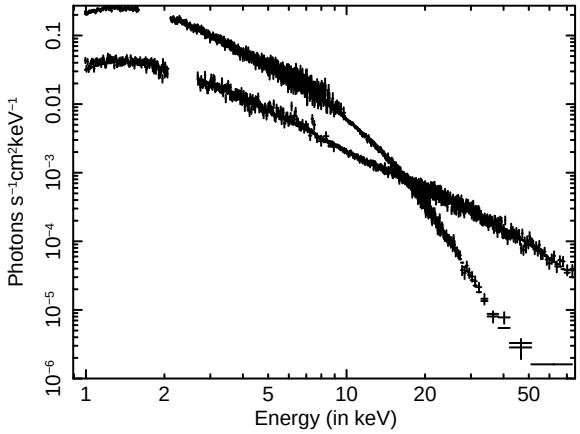


**Figure 4.** In this figure we plot spectra during soft (Obs-2) and hard (Obs-4) state for the comparison

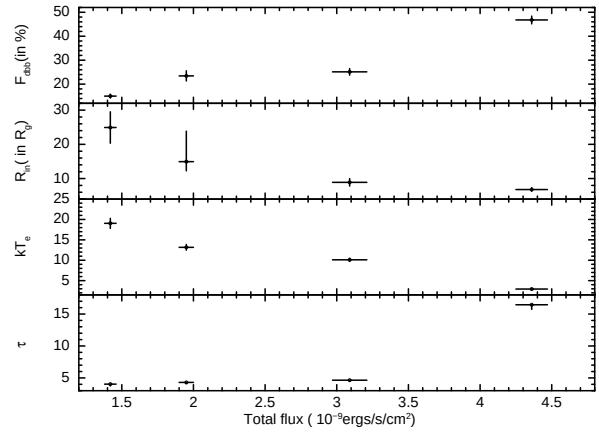


**Figure 5.** Variation of the best fit spectral parameters as function of total (0.1-100 keV) unabsorbed flux. In panel 1 we have also plotted the percentage contribution of disc to the total flux in 0.1-100 keV band.

## 4 DISCUSSION

In this work we present broad band spectroscopy (1-80 keV) of the atoll source 4U 1636-536 using combined NuSTAR and Swift-XRT data. We use a spectral model which has emission component from a standard thin accretion disc,a single temperature blackbody from the hot surface of neutron star and Comptonized emission from the corona. An additional relativistically smeared iron line is also present in all the observations. The model presented in this paper is very similar to the model adopted for this source by Sanna et al. (2013) and Lyu et al. (2014). However, Sanna et al. (2013) use an additional reflection component modeled with BBREFL (reflection of boundary layer photons by accretion disc). The source was found in two different states during the observations: Soft and Hard. Similar state transitions have been reported by Sanna et al (2013) using 6 XMM plus RXTE observations. During the soft state electron temperature was low and optical depth was high. In the hard state, electron temperature was higher and optical depth was lower compared to the soft state. The spectra in the soft state (Obs-2) and in the hard state (Obs-4) are plotted in Figure 4 to show the state transition.

In the soft spectral state of the source we also detect non-thermal tail with photon index $\sim$ 2.4. The source flux was highest in this state ($4.36 \times 10^{-9} ergs/s/cm^2$). The non-thermal component contributes 10% of the unabsorbed 0.1-100 keV flux. Power-law components with photon indices $\sim$ 2-3 contributing 30-80 % of the total flux have been reported during Steep Power-Law state (SPL) of blackhole candidates ( Remillard and McClintock 2006). However, a blackbody emission, probably coming from the boundary layer around neutron star, with temperature in the range 1.2-1.7 keV is also present in the spectra of this source. The presence of boundary layer component suggests that spectral state seen in this source is different from the SPL state of blackhole candidates. A hard tail has been previously reported in this source using the INTEGRAL observation ( Fiocchi et al. 2006). Similar hard tails have been seen previously in Z-sources GX 17+2 (Di Salvo et al. 2000), Cyg X-2 (Di Salvo et al. 2002), Sco X-1 ( D'Amico et al. 2001), GX 349+2 ( Di Salvo et al. 2001) and atoll sources 4U 1705-

44 ( Piraino et al. 2007) and 4U 1728-34 (Tarana et al. 2011).

It has been proposed that hybrid thermal/non-thermal population of electrons in the corona can produce such a hard tail in the neutron star and blackhole binaries ( Poutanen & Coppi 1998). Alternate mechanism such as Comptonization in bulk motion of matter close to the compact object has also been proposed ( Titarchuk and Zannias 1998; Ebisawa, Titarchuk & Chakrabarti 1996). However, Farinelli, Titarchuk & Frontera (2007) suggested that at high accretion rate, radiation pressure due to emission from neutron star surface can slow down the bulk motion of matter causing quenching of bulk Comptonization. Hence the observation of a hard tail at the highest accretion rate suggests that most probably origin of hard tail due to bulk Comptonization is not favourable.

We have detected a broad iron line during all the four observations. The iron emission line profile is well described by a relativistic disc line assuming a Schwarzschild metric. Iron line equivalent width does not show a clear correlation with the flux of Comptonized component (see Table 3) suggesting that dependence may be complex. The inner disc radius obtained from Fe line fit is in the range of $6.5-25GM/c^2$ and is anti-correlated with the observed 0.1-100 keV flux (see Figure 5) . In the soft state it almost extends ($6.5GM/c^2$) upto inner most stable circular orbit. Hence our finding suggests that inner edge of the disc moves inwards as accretion rate increases. We also find that as total observed flux increases contribution of disc flux to the total also increases. The increase in disc fraction implies increase in the seed photon supply for inverse Compton scattering. Hence the corona should cool down and should become compact and optically thick. This is supported by the observed fact that the electron temperature decreases and optical depth increases with increase in the total flux (see Figure 5).

## 5 CONCLUSION

Investigation of broad band X-ray spectra of the source revealed the presence of a non-thermal component and a broad iron line. The source exhibited flux and state variations during the observations. The spectral parameters showed significant evolution as the persistent flux level of source varied. Finally, we have proposed a scenario which explains the spectral evolution of the source.

## ACKNOWLEDGMENTS

This research has made use of data and/or software provided by High Energy Astrophysics Science Archive Research Center (HEASARC). We thank Dr. Anil Agarwal, GD, SAG, Mr. Subramanya Udupa. DD, CDA and Dr. M. Annadurai, Director, ISAC for encouragement and continuous support to carry out this research.

## REFERENCES

Agrawal V.K., Misra R., 2009,MNRAS,398,1352
Agrawal V.K., Sreekumar P., 2003,MNRAS,346,933
Arnaud K.A., and Dorman B.,2000,XSPEC is available via the HEASARC on-line service,provided by NASA/GSFC
Barret D., 2001,AdSpR,28,307
Barret D., Olive J.F., Boirin L.,Done C.,Skinner G.K, Grindlay J.E., 2000,ApJ, 533,329
Casares J., Cornelisse R., Steeghs D., Charles P.A., Hynes R.I.,O'Brien K.,Strohmayer T.E.,2006, MNRAS,373,1235
Chiang Chia-Ying, Morgan R.A., Cackett E. M., Miller J.M., Bhattacharyya S., Strohmayer T.E., 2016, ApJ,831,45
D'Amico F.,Heindl W.A.,Rothschild R.E., Gruber D.E., 2001, ApJ, 547,L147
Degenaar N., Miller J.M., Chakrabarti D., Harrison F.A., Kara E., Fabian A.C., 2015, MNRAS Letters,451,85
Di Salvo T., Stella L.,Robba N.R., van der Klis M., Burderi L., Israel G.L, Homan J.,Compana S. et al., 2000, ApJ, 544, L119
Di Salvo T., et al., 2001,ApJ,554,49
Di Salvo T. et al., 2002, A&A, 386, 535
Done C., Gierlinski M., Kubota A., 2007, A&A Rev., 15,1
Ebisawa K., Titarchuk L., & Chakrabarti S.K.,1996,PASJ,48,59
Fabian A.C., Rees M. J., Stella L., & White N.E., 1989,MNRAS, 238, 729
Farinelli R., Titarchuk L., & Frontera F., 2007, ApJ, 662,1167
Fioochi M., Bazzano A., Ubertini P., 2006, ApJ, 651,416
Galloway D. K., Psaltis D., Muno M.P., Chakrabarti D., 2006,ApJ,639, 1033
Giles A.B., Hill K.N., Strohmayer T.E., Cummings N., 2002,ApJ,568, 279
Hasinger G., van der Klis M., 1989, A&A, 225, 79
Lyu M., Mendez M., Sanna A., Homan J., Belloni T., Hiemstra B., 2014, MNRAS, 440, 1165
Miller J.M.,2007,ARA&A, 45,441
Miller J.M., Parker M.L., Fuerst F., Bachetti M, Barret D., Grefenstette B.W., Tendulkar S., Harrison F.A., et al., 2013, ApJL,779,2
Mitsuda K., Inoue H., Nakamura N., Tanaka Y., 1989, PASJ, 41, 97
Mitsuda K., et al., 1984, PASJ, 36, 741
Piraino S., Santangelo A., Di Salvo T., Kaaret P., Horns D., Iaria R., Burderi L., 2007, A&A, 471,L17.
Piraino S., Santangelo A., Ford E.C., Kaaret P., 1999, A&A, 349, 77
Poutanen J., & Coppi P.S., 1998, Phys, Scr, T77,57
Remillard R.A. & McClintock J.E. 2006, ARA&A, 44,49
Reynolds C.S., Nowak M.A., 2003,Phys. Rep.,377,389
Sanna A., Hiemstra B., Mendez M., Altamirano D., Belloni T., Linares M., 2013, MNRAS, 432, 1144
Sleator C.C., Tomsick J.A., King A.L., Miller J.M., Boggs S.E., Bachetti M., Barret D., Chenevez J., 2016, ApJ, 827,134
Strohmayer T.E., Markwardt C.B., 2002, ApJ,577,337
Sunyaev R.A., Titarchuk L., 1980, A&A, 86, 121
Tarana A., Belloni T., Bazzano A., Mendez M. and Ubertini P., 2011, MNRAS,416,873
Tarana A., Bazzano A., Ubertini P., 2008, ApJ,688,1295
Titarchuk L. & Zannias T., 1998, ApJ, 493,863
Titarchuk L., 1994, ApJ, 434,570
Wijnands R. A. D., van der Klis M., Van Paradijs, Lewin W.H.G., Lamb F.K., Vaughn B., Kuulkers E., 1997, ApJ,

479, L141
Wilms J., Allen A., McCray R., 2000,ApJ,542,914
Zdziarski A. A., Johnson W.N., Magdziarz P., 1996, MNRAS,283,193
Zycki P.T., Done C., Smith D.A., 1999, MNRAS, 309,561